

## Electronic Supplementary Information

Fei Liu<sup>1</sup>, Na Yang<sup>1,\*</sup>

1. State Key Laboratory of Medicinal Chemical Biology, College of Pharmacy and Key Laboratory of Medical Data Analysis and Statistical Research of Tianjin, Nankai University, 300353 Tianjin, China

\* yangnanku@nankai.edu.cn

### 1 Method and Model

To capture the conformational change of SIRT1 during the process of the activation process of it, we modified the traditional structure based energy hamiltonian by integrating information of the open(PDB:4ZZJ) and closed structures(PDB:5BTR). We built a residue-level two-basin structure-based model and the Hamiltonian is given by the expression:

$$U_{total}(\Gamma_{open}, \Gamma_{closed}) = U_{Local} + U_{Attraction} + U_{Repulsive}$$

In this model, each amino acid in SIRT1-P53 complex was represented by one bead CA. The residue in backbone was represented by the CA bead, which was located on the  $C_{\alpha}$  atom.

#### 1.1 Construction of mixture contact map

We built a mixed contact map to integrate two structural information together. The native contact gives all possible interactions between pairs of residues in a given structure. In this work, the native SIRT1 contacts were defined by contact map obtained with CSU algorithm[1]. We integrated a mixed contact map into this model by  $U_{Attraction}$  in Hamiltonian energy. The  $U_{Attraction}$  is give by the expression:

$$\begin{aligned} U_{Attraction} &= U_{LJ}(Core) + U_{LJ}(open) + \\ &U_{LJ}(closed) + U_{LJ}(STAC) \\ &= \epsilon_{Core}U_{LJ} + \epsilon_{Specific}(\epsilon_{open}U_{LJ} + \epsilon_{closed}U_{LJ}) + \\ &\epsilon_{STAC}U_{LJ} \\ U_{LJ} &= \epsilon_{LJ}[5(\frac{\sigma_{ij}}{r_0})^{12} - 6(\frac{\sigma_{ij}}{r_0})^{10}] \end{aligned}$$

The  $\epsilon_{Core} = 1.2$ ,  $\epsilon_{Specific} = 1.0$ ,  $\epsilon_{open} = 1.0$ ,  $\epsilon_{closed} = 0.9$ ,  $\epsilon_{STAC} = 1.0$ . Because the region of Core should be under less conformational change than the specific region, we set the  $\epsilon_{Core}$  to 1.2, which is larger than  $\epsilon_{Specific}$  1.0. In addition, the initial term of  $U_{Local}$  of the model is depended on the closed structure except rescaling the hinge region(the detail of hinge region is in the subsection Local Potential and the Flexibility of Hinge Regions ). So the  $\epsilon_{closed}$  depended on the closed structure is set to a smaller value than the  $\epsilon_{open}$  depend on the open structure(0.9 VS 1.0) to balance the bias on closed state. The concrete details of building the mixed contact map are given as follows.

##### 1.1.1 Total contact library $\gamma^{all}$

We build a contact library by collecting all the pairs in the contact map obtained from the reference crystal structures(4ZZJ,5BTR). There are 1170 contacts.

##### 1.1.2 Reference distances

We calculate the distances  $r_{ij}^{open}$  and  $r_{ij}^{close}$  between the two beads i and j in the library.  $r_{ij}^{open}$  and  $r_{ij}^{close}$  represent the distance of the bead in open state and close state, respectively.

##### 1.1.3 Core sublibrary $\gamma^{Core}$

We defined  $R_{ij}(X/Y) = \frac{r_{ij}^X}{r_{ij}^Y}$ . For a bead pair between i and j, if both  $R_{ij}(open/closed)$  and  $R_{ij}(closed/open)$  are less than  $R_{cut}$ , this pair will be considered as a member of core contact library ( $\gamma^{Core}$ ). We used  $R_{cut} = 1.25$  in present work. 1120 contacts were obtained in the sublibrary  $\gamma^{Core}$ . The contacts in  $\gamma^{Core}$  is shared by open and closed states

##### 1.1.4 State-open sublibrary $\gamma^{open}$

For a pair with  $R_{ij}(open/closed) > R_{cut}$ , it will be considered as a member of state-open contact library  $\gamma^{open}$ . We used  $R_{cut} = 1.4$  here. There were 9 contacts in  $\gamma^{open}$ .

##### 1.1.5 State-closed sublibrary $\gamma^{closed}$

For a pair with  $R_{ij}(closed/open) > R_{cut}$ , it will be considered as a member of specific contacts in closed state. The number of specific contacts in closed state is are 24.

##### 1.1.6 STAC-mediated sublibrary $\gamma^{STAC}$

We introduce a implicit STAC into the simulation by adding selected STAC-mediated interactions to the structured based potential, an approach that has been used before in the coarse grained simulation[7,8]. Finally, we identified STAC-mediated interactions.

##### 1.1.7 Repulsive interactions

The  $\sigma_{NC}$  is the excluded distance between non-native pairs to provide excluded volume repulsion. The repulsive rail is  $4.0 \text{ \AA}$ , the  $\epsilon_{NC} = 1KJ/mol$ . All pairs in  $\gamma^{all}$  were not considered in this term.

$$U_{Repulsive} = \epsilon_{NC}(\frac{\sigma_{NC}}{r_{ij}})^{12}$$

$$U_{Electrostatic} = \epsilon_E K_{coulomb} B(K) \frac{q_i q_j \exp(-kr_{ij})}{\epsilon_r r_{ij}}$$

### 1.1.8 Local Potential and the Flexibility of Hinge Regions

The Local potential is divided into bond stretching, angle bending, torsion energy. The bonded energies  $U_{Bonds}$  are summed over the energy of all co-valent bonds.  $K_r = 10000KJ/(mol\ nm^2)$  is the bond constant. The angle constant  $K_\theta = 20kJ/mol$ . The  $K_\phi = 0.8kJ/mol$ .  $U_{Local} = U_{Bonds} + U_{Angles} + U_{Dihedrals}$

$$U_{Bonds} = \sum_{bonds} K_b(r - r_0)^2 = 0$$

$$U_{Angles} + U_{Dihedral} = \epsilon_{angle}(U_{Non-hinge} + \epsilon_{Hinge}U_{Hinge})$$

$$U_{Non-hinge} = K_\theta(\theta - \theta_0)^2 + K_\phi[(1 - \cos(\phi - \phi_0)) + 0.5(1 - \cos(\phi - \phi_0))]$$

$$U_{Hinge} = K_\theta(\theta - \theta_0)^2 + K_\phi[(1 - \cos(\phi - \phi_0)) + 0.5(1 - \cos(\phi - \phi_0))]$$

Previous theoretical investigations reported that large-amplitude conformational change may cause structural strain in specific portions of the protein (such as the hinge region). It is assumed that the strong local strain energies could be released by breaking fragile local interactions. The local interactions were weakened by decreasing the site-specific constants  $\epsilon_{Hinge}$  as in the previous two-basin model. The regions of the hinge are determined by the angle differences of pseudo angle and pseudo dihedral between open state and closed state. Hinges were located wherever pseudo angle or pseudo dihedral angle differences were greater than threshold values. The threshold values of pseudo angle and pseudo dihedral are  $10^\circ$  and  $20^\circ$ , respectively. Because of the hinge region has large amplitude conformational change, it may cause structural strain which can lead to the local energy release. In this model, we release the energy by breaking the fragile local interactions [2]. We weaken it by decreasing the site-specific constants. We adopt the similar strategy just as the previous studies[2]. The site-specific constant was rescaled by  $\min(1, C_\theta/E_{\theta_i})$ , where the threshold  $C_\theta = 1.0$ ,  $E_{\theta_i} = K_\theta * |\theta_O - \theta_C|^2$ . Similarly, we rescaled the site-specific constants for the dihedral angle, by  $\min(1, C_\phi/E_{\phi_i})$ , in which the thresholds were set as  $C_\phi = 1.0$ ,  $E_{\phi_i} = K_\phi * [1 - \cos(|\phi_O - \phi_C|) + 0.5(1 - \cos(3|\phi_O - \phi_C|))]$

### 1.2 Fraction of formation of certain state-specific contacts

The traditional folding Q has been a exact reaction coordinate in measuring the degree of folding in the studies of protein folding[3]. However, for functional dynamics, most contacts are shared by the native functional states, which will not be broken in the process of functional dynamics. Therefore, we should only measure the formation of state-specific contacts(See **Construction of mixture contact map**) instead of all native contacts to describe the functional landscape. The Q of state-specific contacts ha the same definition

with the Q of all contacts, which has been successfully used in other studies[4-6]. The difference is that they can describe the folding degree of different regions. It can be expressed by:

$$Q_{open,closed,STAC}$$

$$= \sum_{\gamma_{open,closed,STAC}} \frac{1 - ((R_{ij} - D_0)/R_{ij}^{nat})^n}{1 - ((R_{ij} - D_0)/R_{ij}^{nat})^m}$$

where,  $m = 20$ ,  $n = 10$ ,  $R_{ij}^{nat}$  is native distance of atom i and atom j.  $D_0 = 0.3 * R_{ij}^{nat}$ . Furthermore, we defined the average specific native contact of each residue. It can be expressed by:

$$(AQ_{open,closed,STAC})_j$$

$$= \sum_i (Q_{open,closed,STAC})_{ij}$$

## References

- [1] Sobolev V, Sorokine A, Prilusky J (1999) Automated analysis of interatomic contacts in proteins. *Bioinformatics*15, 327–32
- [2] Okazaki, K, Koga, N, Takada, S, Onuchic, J. N, Wolynes, P. G. (2006) Multiple-basin energy landscapes for large-amplitude conformational motions of proteins: Structure-based molecular dynamics simulations. *Proc Natl Acad Sci U S A*103, 11844–9.
- [3] Cho, S. S, Levy, Y, Wolynes, P. G. (2006) P versus q: structural reaction coordinates capture protein folding on smooth landscapes. *Proc Natl Acad Sci U S A*103, 586–591.
- [4] Wang J, Wang Y (2011) Multi-scaled explorations of binding-induced folding of intrinsically disordered protein inhibitor ia3 to its target enzyme. *PLoS Comput Biol*7, e1001118.
- [5] YaoX Q, Kenzaki H, Murakami S, Takada S(2010) Drug export and allosteric coupling in a multidrug transporter revealed by molecular simulations. *Nat Commun*1, 117.
- [6] Jana B, Adkar, B. V, Biswas, R, Bagchi, B. (2011) Dynamic coupling between the lid and nmp domain motions in the catalytic conversion of atp and amp to adp by adenylate kinase. *J Chem Phys*134, 035101.
- [7] Whitford, P.; Miyashita, O.; Levy, Y.; Onuchic, J. N. Conformational transitions of adenylate kinase: Switching by cracking. *J Mol Biol* 2007, 366(5), 16611671.
- [8] Daily MD, Phillips GN, Cui QA. (2010) Many local motions cooperate to produce the adenylate kinase conformational transition. *J Mol Biol* 400, 618-631.

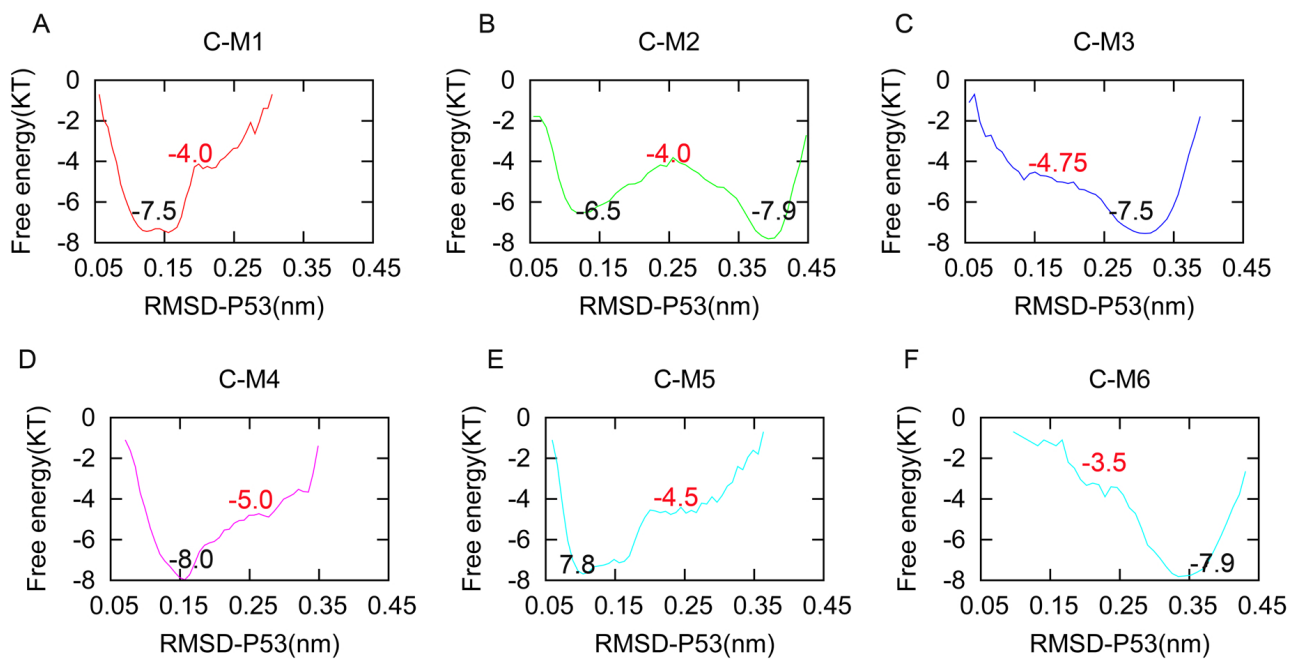


Fig. S 1: The 1D landscapes from model C-M1 to C-M6 are shown from figure A to figure F. The RMSD-P53 are root-mean-square deviation of the SIRT1 and root-mean-square deviation of the P53 peptide relative to the native SIRT1/FdL peptide/resveratrol structure (PDB: 5BTR)

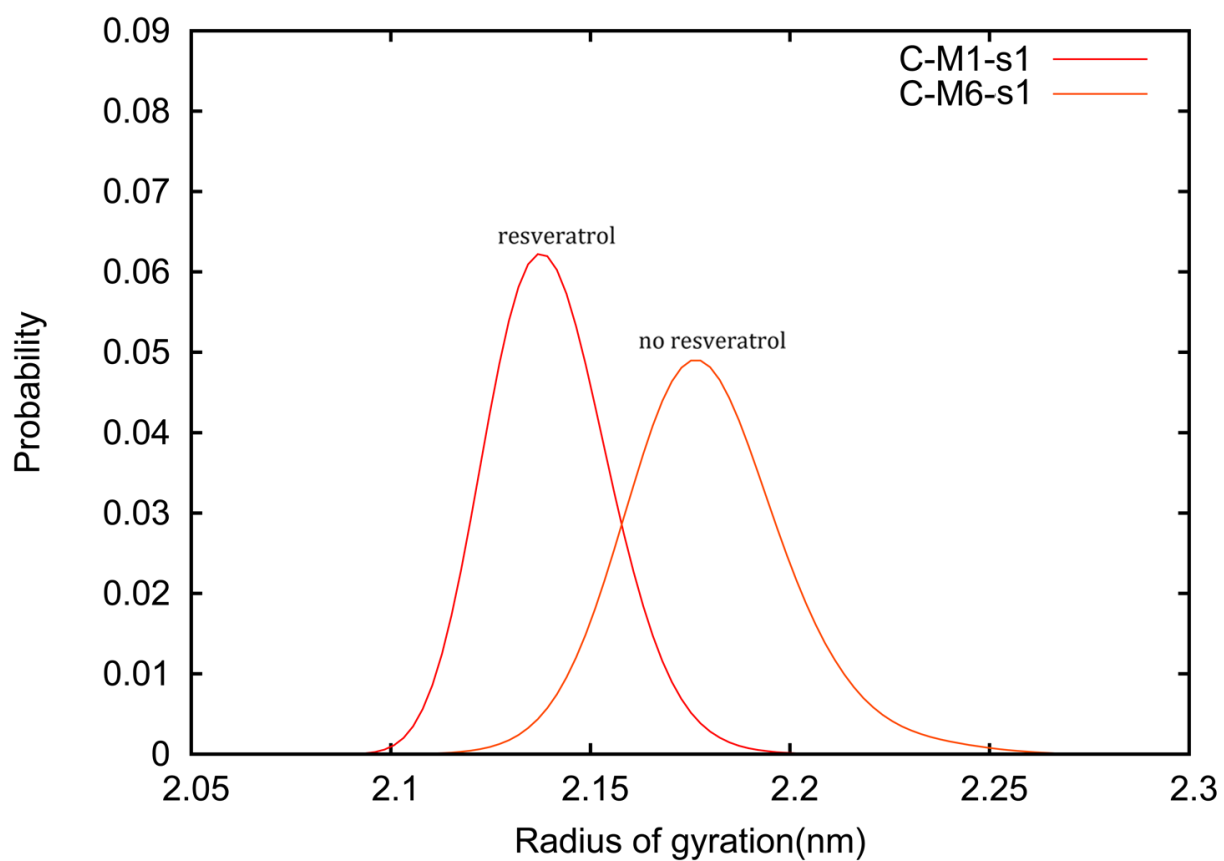


Fig. S 2: The distribution of the radius of gyration of the conformation of SIRT1 in states C-M1-S1(Including three resveratrols) and C-M6-S1(no resveratrol) are shown, respectively. It shows that the SIRT1 has more compact conformation under the binidng of resveratrol.

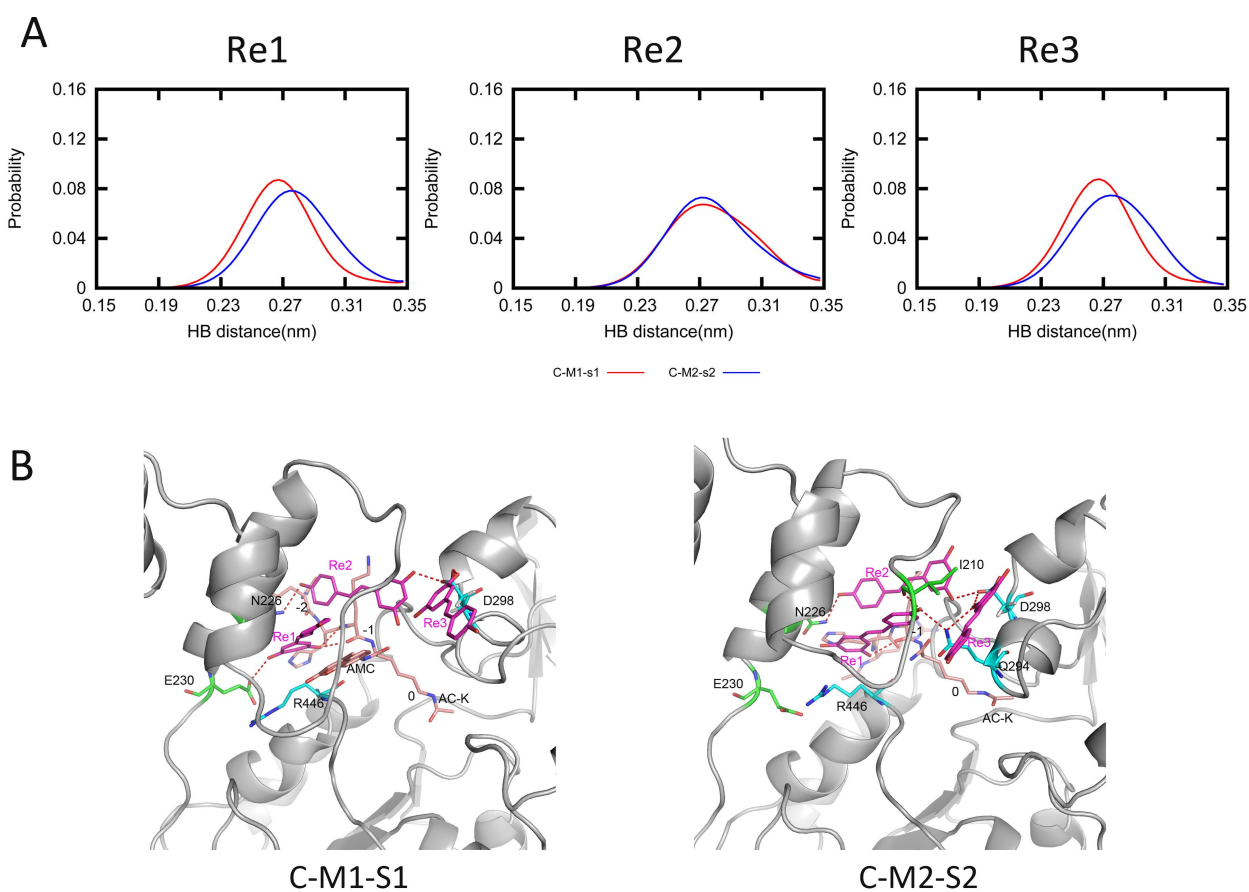


Fig. S 3: (A) The distance distribution of the hydrogen bonds (HB distance) between the SIRT1 and three resveratrols (Re1, Re2 and Re3). The red line shows HB distance distribution of model C-M1, which included an AMC-p53 peptide. The blue line shows HB distance distribution of model C-M2, which included a no-AMC p53 peptide. (B) The structures representing the hydrogen bond between the SIRT1 and resveratrols in states C-M1-S1 and C-M2-S2 are shown, respectively. Resveratrol is colored magenta; p53 and no-AMC-p53 are colored salmon; residues N226 and E230 are colored green; and residue R446 is colored cyan. Hydrogen bonds are shown by a red dotted line.

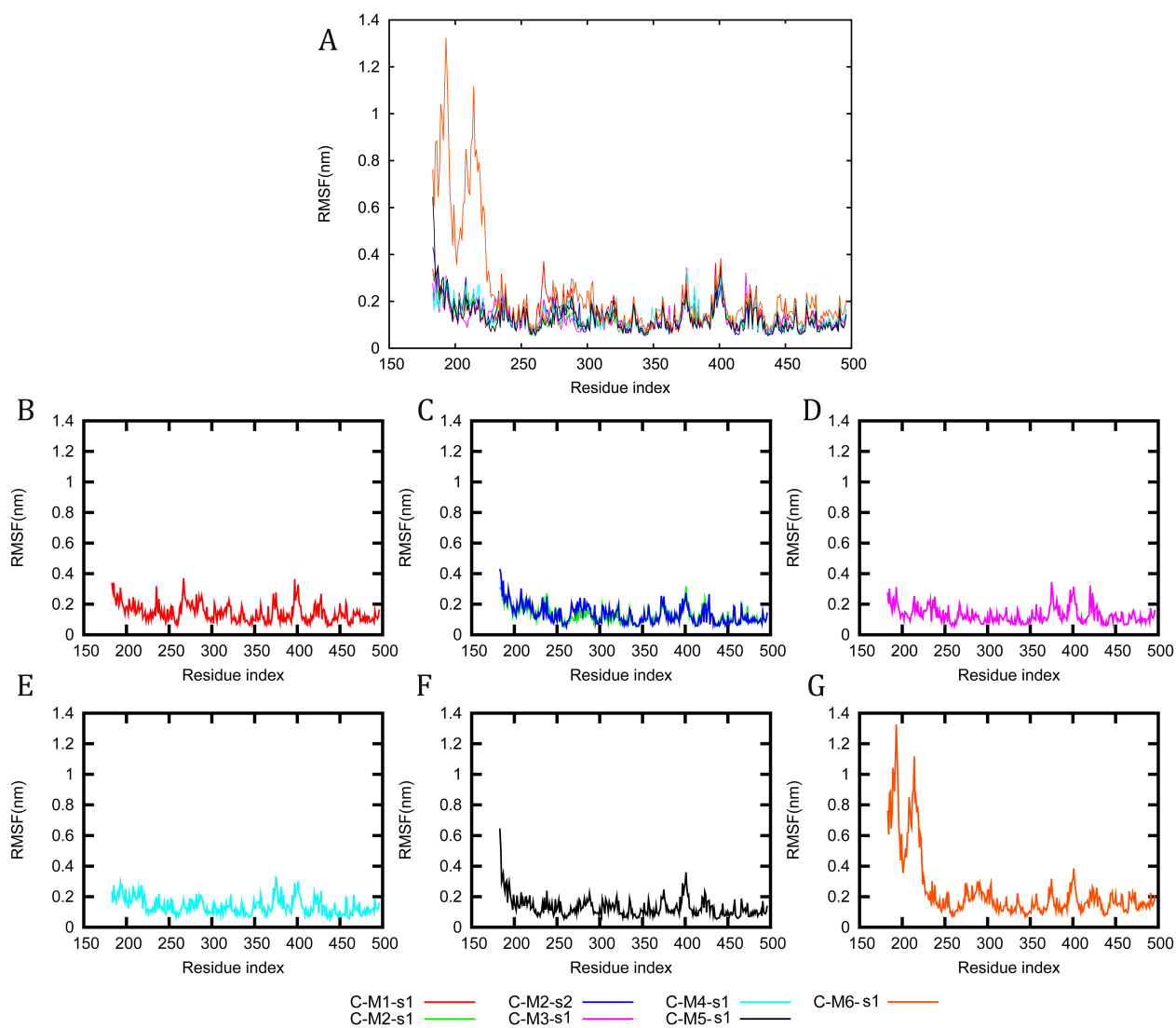


Fig. S 4: The root mean square fluctuation(RMSF) of the conformation of SIRT1 in different states are shown from subfigure A to subfigure G. (A)The root mean square fluctuation of the conformation of SIRT1 in all states are shown. (B-G) The root mean square fluctuation of the conformation of SIRT1 in different states are shown in different colors, respectively. Red: C-M1-S1; Green: C-M2-S1; Blue: C-M2-S2; Magenta: C-M3-S1; Cyan: C-M4-S1; Black: C-M5-S1; Orange: C-M6-S1.

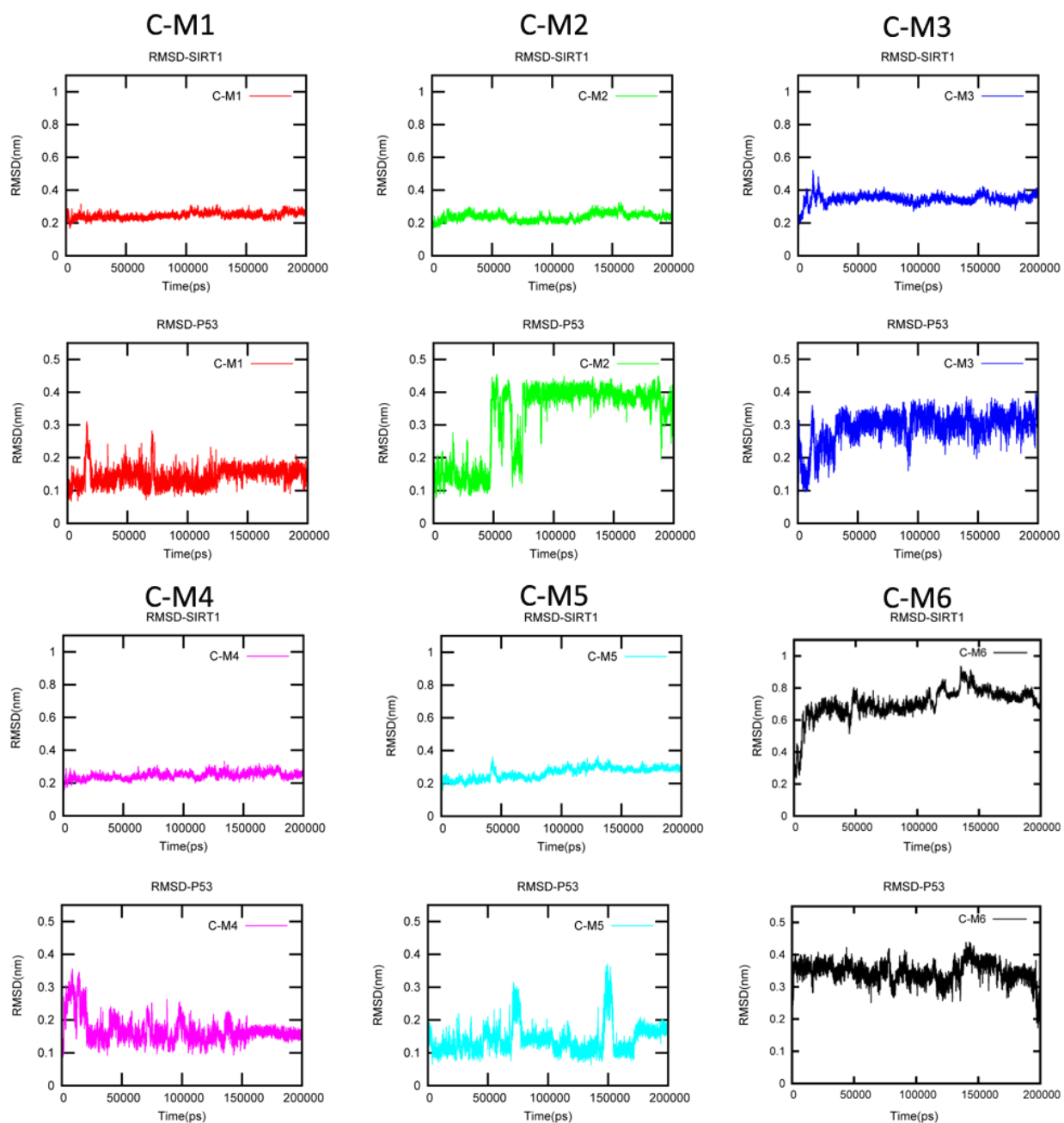


Fig. S 5: The trajectories of root mean square deviation of the SIRT1 relative to the native 5BTR model of C-M1 to C-M6 are shown, respectively.

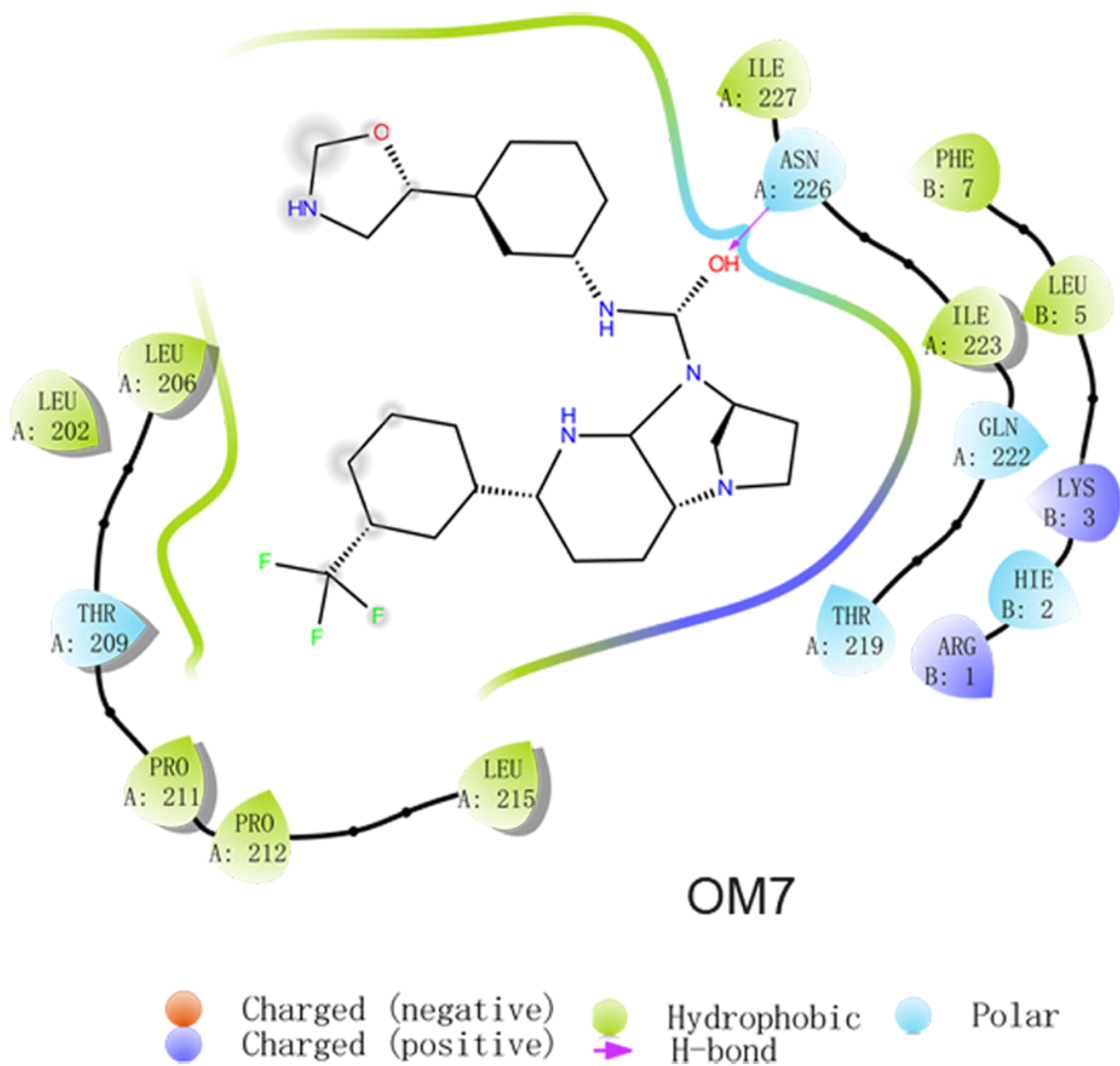
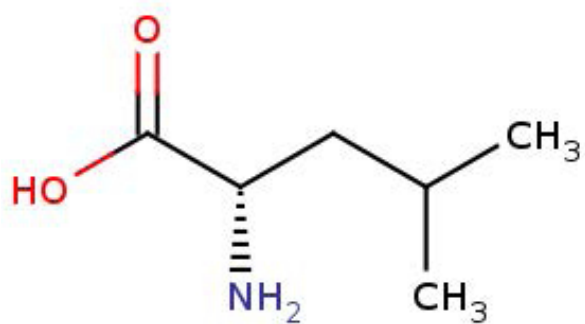
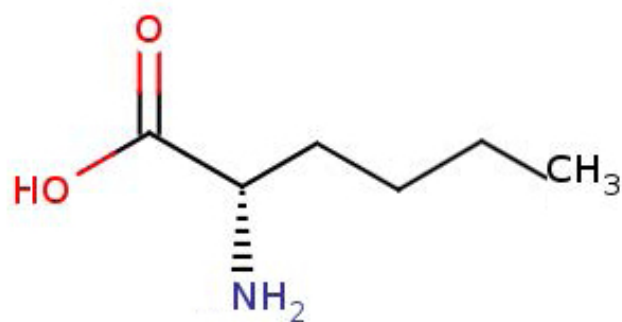


Fig. S 6: Binding models of SIRT1, STAC-1, and p53 peptide in the final state of OM7, respectively. SIRT1 and p53 are represented by chains A and B, respectively, and STAC-1 is shown as its structural chemical formula. The residues are colored according to their properties (red: negative charge; blue: positive charge; cyan: polar; green: hydrophobic; magenta arrow: hydrogen bond).



LEU



NLE

Fig. S 7: The chemically structural formula of LEU and NLE are shown, respectively.